Chemical Engineering Journal 421 (2021) 129905

Contents lists available at ScienceDirect

Chemical Engineering Journal

journal homepage: www.elsevier.com/locate/cej

Significantly enhanced desalination performance of flow-electrode capacitive deionization via cathodic iodide redox couple and its great potential in treatment of iodide-containing saline wastewater

Kunyue Luo [a,b,1], Ming Chen [c,1], Wenle Xing [a,b], Mengbiao Duan [a,b], Jiaxin Du [a,b], Guangming Zeng [a,b,*], Wangwang Tang [a,b,*]

[a] *College of Environmental Science and Engineering, Hunan University, Changsha 410082, China*
[b] *Key Laboratory of Environmental Biology and Pollution Control (Hunan University), Ministry of Education, Changsha 410082, China*
[c] *Key Laboratory of Reservoir Aquatic Environment, Chongqing Institute of Green and Intelligent Technology, Chinese Academy of Sciences, Chongqing 400714, China*

ARTICLE INFO

Keywords:
Capacitive deionization
Water desalination
Ion removal
Iodide-containing saline wastewater

ABSTRACT

Flow-electrode capacitive deionization (FCDI) is attracting growing attention owing to its advantages such as effective ion removal capacity and easy management of the electrodes. Optimization of the flow-electrode comprising carbon materials and aqueous electrolyte is always a research hotspot aimed at improving FCDI performance. Herein, we innovatively introduced appropriate amount of KI_3 into the cathodic flow-electrode to provide a highly efficient means of enhancing FCDI desalination performance with a stable behavior in salt electrosorption and desorption over multi-cycle consecutive runs. The accelerated salt removal rate originated from the reversible redox reaction of I_3^-/I^- and the maintenance of the electro-neutrality of the global electrolyte. Although possible minor release or leakage of I^-/I_3^- through the cation-exchange membrane and into the treated water occurred, which makes the proposed approach not quite suitable for potable water production, we demonstrated that this system has great application prospects in treatment of iodide-containing saline wastewater without causing secondary pollution.

1. Introduction

Freshwater scarcity and water pollution are two of the most important environmental problems faced by human beings in the 21st century, which necessitates a continuing search for eco-friendly and cost-effective technologies for water desalination and wastewater treatment [1–7]. Capacitive deionization (CDI) is an emerging technology mainly suited for such applications including desalination and removal of ionic contaminants from water [4–11]. CDI functions by adsorbing ions in the electric double layers of capacitive electrodes via electrostatic interaction or in the inner structures of battery electrodes via Faradaic intercalation [4–16]. Among the various cell configurations within the CDI community, flow-electrode CDI (FCDI) involving the use of flowable carbon or composite electrodes stands out and attracts increasing attention due to its key advantages of facile electrode preparation, continuous desalting behavior, excellent salt removal efficency (95%, NaCl solution: 32.1 g L^{-1}) and high water recovery rate (greater than95%) [17–25]. Under an electric field, ions in the feed water would pass through ion exchange membrane and enter the anodic or cathodic chamber of FCDI whereby they would be eventually adsorbed on the suspended carbon particles or retained in the aqueous phase of the flow electrode [19,21].

Despite the distinct advantages of FCDI, it suffers from a major limitation, i.e., the inefficient charge transfer between the current collectors and flow electrodes owing to the discontinuous conductive electrical network of the suspended active materials in the flow-electrode slurry [19,21,23]. Although increasing carbon content or introducing carbon black facilitates electron transport, the viscosity of the flow electrode rises accordingly, which might result in electrode-channel clogging [19,26–29]. Performing chemical surface treatment of carbon particles to lower the viscosity of carbon slurry, and, as a result, to increase the carbon mass loading to a very high value (e.g., 35 wt% activated carbon content) without channel clogging is an effective method to solve this limitation [27,30]. However, such surface

---

* Corresponding authors at: College of Environmental Science and Engineering, Hunan University, Changsha 410082, China.
E-mail addresses: zgming@hnu.edu.cn (G. Zeng), wtang@hnu.edu.cn (W. Tang).

[1] These authors contribute equally to this article.

https://doi.org/10.1016/j.cej.2021.129905
Received 15 February 2021; Received in revised form 8 April 2021; Accepted 13 April 2021

modification processes are somewhat costly (requiring use of chemicals such as nitric acid, sodium hydroxide or sodium 4-vinylbenzenesulfonate), and time- and labor-consuming (usually undergoing the processes of chemical modification, repeated washing with ultrapure water, and drying). Raising electrolyte concentration in the slurries is also beneficial to enhancing the flow-electrode conductivity and thereby the desalting efficiency [31], but the degree of performance improvement is very limited and significant concentration polarization at the membrane interface and aggregation of carbon particles might occur [31,32].

Consideration is given in this work to an alternative route of accelerating electron flow via addition of redox-active substance to the flow electrodes. Ma et al. previously proposed the use of a redox-active flow-anode containing hydroquinone/benzoquinone couple to achieve a significantly improved FCDI desalination performance [32]. Nevertheless, a critical concern arose from the permeation of toxic hydroquinone/benzoquinone couple through the ion exchange membrane into the treated water stream. Wang et al. achieved enhanced desalination performance of a FCDI system via addition of vanadium redox couples (V^{2+}/V^{3+}) into the activated carbon flow-electrode [33]. However, vanadium compounds are generally expensive, which restricts their practical applications. It is of great importance to find a more suitable redox-active electrolyte for the flow electrode. Iodide-based redox electrolyte comprising I^-/I_3^- couple has been reported to possess promising performance in the field of electric energy storage and water desalination [34–37], but these studies are based on the use of redox-active electrolyte only in the absence of carbon. No study is yet available exploring its effects on the ion removal process in an FCDI system. Iodide, an essential micronutrient for life, is readily available and is considered to have low toxicity and low cost [36]. Moreover, it is expected that the cation exchange membrane (CEM) could inhibit the diffusion of I^-/I_3^- couple into the treated water stream when iodide-based redox electrolyte is only employed in the cathodic flow-electrode.

Therefore, in this work, we aimed to investigate the efficacy of applying iodide-based redox electrolyte in the cathodic chamber of FCDI in promoting both salt electrosorption and desorption processes with the underlying mechanisms involved also analyzed. Considering the possibly unavoidable leakage/release of iodine into the treated water stream, we further investigated the potential of this method in treatment of iodide-containing saline wastewater.

2. Materials and methods

The structure and components of FCDI cell used in this study were described in detail in the Supporting Information. Isolated closed-cycle (ICC) batch-flow operational mode was used for the whole experiment as shown in Fig. S2, i.e., 100 mL positively and negatively charged flow electrodes were individually recycled between the FCDI cell and stirred reservoir at a flow rate of 50 mL min^{-1}, while the feed water requiring desalination (50 mL of 3 g L^{-1} KCl solution) was recirculated at a flow rate of 25 mL min^{-1}. The cathodic redox-active carbon slurry consisted of 5 wt% activated carbon powder (No. 10006619, Sinopsin Chemical Reagent Co., Ltd., China), 1 wt% carbon black (LION Ketjenblack, ECP600JD, Japan) and certain concentrations of KCl and KI_3 solution. We defined the concentration of KI_3 used during the experiment according to $I^- + I_2 \leftrightarrow I_3^-$. For example, 12 mM KI_3 (actually smaller than 12 mM) was prepared by dissolving 0.3 g I_2 and 0.2 g KI in 100 mL ultrapure water. Correspondingly, the carbon slurry without KI_3 and the redox-active electrolyte without carbon were used as the control groups. The anodic flow electrode was composed of 5 wt% activated carbon, 1 wt% carbon black and certain concentration of KCl solution. Iodide-containing saline wastewater was simulated by dissolving appropriate amount of KCl, KNO_3, Na_2SO_4, KBr and KI in ultrapure water. Prior to each experiment, the electrode chambers and spacer channels were rinsed thoroughly with ultrapure water to ensure no impact of the previous test on the next one, and then the water remaining in the FCDI device and tubes was evacuated. In the case of cycling the flow-electrodes and feed water, the electrical circuit was not connected until the conductivity reading of the feed water became stabilized. In one cycle, electrosorption was carried out at a constant charging voltage using a direct-current power supply, followed by a reversed voltage of the same value for desorption. After electrode regeneration, the polarity of the electrodes was reversed to initiate the next cycle. The electrical conductivity and pH were monitored using the conductivity meter (DDS-307, INESA Scientific Instrument Co., Ltd, China) and pH meter (PHS-3C, INESA Scientific Instrument Co., Ltd, China), respectively. The current flowing through the FCDI cell was measured using a current probe connected to a data acquisition system (SensorDAQ, Vernier, USA).

The specific surface area, pore size and pore volume of the activated carbon were determined using a Micromeritics ASAP-2020 Accelerated Surface Area and Porosimetry Analyzer based on N_2 adsorption/desorption isotherm. All samples were filtered through 0.45 μm filters prior to further analysis. The concentrations of total iodine and K^+ were measured by inductively coupled plasma mass spectrometry (ICP-MS) and the concentrations of I^- and Cl^- were measured by ion chromatograph. Through the mass balance principle, the amount of specific ions (e.g., K^+) adsorbed on cathodic carbons during charging was calculated based on the difference between the total K^+ concentration in the system and the sum of K^+ concentrations in the cathodic aqueous solution, the treated stream and the anodic aqueous solution (we neglected the amount of K^+ adsorbed on anodic carbons).

The cyclic voltammetry (CV) and electrochemical impedance spectroscopy (EIS) tests were conducted in a three-electrode system by using a CHI760E electrochemical workstation (Shanghai, China) with Ag/AgCl as the reference electrode, Pt as the working electrode and counter electrode (each Pt electrode size: 0.9 cm × 1.5 cm). The working, counter and reference electrodes were immersed into 100 mL suspension of carbon particles consisting of 5 wt% activated carbon, 1 wt% carbon black, 1000 mg L^{-1} KCl and initial concentrations (0 mM or 12 mM) of KI_3 with a stirring rate of 1000 r/min. CV analysis was carried out with a scan rate of 10 mV/s and voltage window varying from − 1.2 to 1.2 V. EIS measurements were run in the frequency charging from 0.1 Hz to 10^4 Hz by applying a small alternating current signal with an amplitude of 10 mV.

The ion removal efficiency was calculated according to the following equation,

$$\text{Removalefficiency}(\%) = \frac{C_0 - C_t}{C_0} \times 100 \tag{1}$$

where C_0 and C_t (mg/L) represent the initial and final concentrations of the specific ion in the feed water, respectively.

3. Results and discussion

3.1. Effects of electrolyte concentration in the flow electrode on deionization

One previous research indicated that the desalination performance of FCDI operated in short-circuited closed-cycle mode increased with increments of NaCl concentrations in the flow-electrode at a low NaCl concentration region of 0.00–1.48 wt%, and the desalting efficiency remained almost constant when the aqueous NaCl electrolyte in the flow-electrode was greater than 1.48 wt% [31]. To determine whether the saturation point also existed for FCDI operated in isolated closed-cycle mode in this study, we firstly investigated the temporal variation of conductivity of the treated salty water by varying electrolyte (KCl) concentrations (0, 1000, 2000, 3000, 5000 mg L^{-1}) in both of the flow electrodes without addition of iodide redox couple with the results shown in Fig. 1. As can be seen, the desalination performance of FCDI was improved when the flow-electrode was prepared with 1000 mg L^{-1} KCl electrolyte instead of ultrapure water largely due to the decrease in

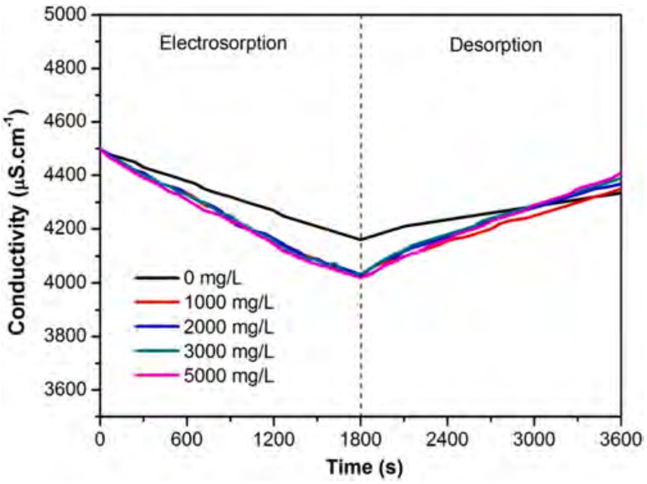

Fig. 1. Dynamic variation in conductivity of the treated salty water during electrosorption and desorption as a function of varying initial electrolyte (KCl) concentrations in the flow-electrodes without iodide redox couple. Feed solution: 3000 mg L^{-1} KCl; Charging voltage: 1.2 V; Discharging voltage: −1.2 V.

the resistance of the flow electrode chamber, while the desalting efficiency of the flow-electrodes with KCl concentrations ranging between 1000 mg L^{-1} and 5000 mg L^{-1} kept nearly unchanged attributed to the existence of sufficient KCl salt in the flow-electrode. Therefore, we can consider that, at 1000 mg L^{-1} KCl concentration, the desalting efficiency of the flow electrodes reached saturation. To exclude the effect of electrolyte concentration in the flow electrode on deionization when iodide redox couple was added into the cathodic flow-electrode, we further conducted experiments by varying initial KCl concentration of the cathodic flow-electrode from 1000 to 5000 mg L^{-1} while fixing initial KCl concentration of the anodic flow-electrode at 1000 mg L^{-1}, and we also observed insignificant variation in the conductivity of the treated salty water versus time. Based on the above results, 1000 mg L^{-1} KCl was selected for preparing the flow electrodes for subsequent studies.

3.2. *Desalination performance affected by introduction of iodide redox couple in cathodic flow-electrode and the underlying mechanisms*

The influence of the addition of KI_3 into the cathodic flow-electrode on the desalination performance of FCDI was presented in Fig. 2a, from which it can be observed that, after a charging voltage was applied across the cell, much more rapid salt removal occurred in the FCDI containing KI_3 compared with that without KI_3, with a similar positive effect noticed during desorption upon polarity reversal. Additionally, the salt removal efficiency increased with an increase in the amount of KI_3 added to the cathodic flow-electrode ranging from 0 to 12 mM. Specifically, under initial KI_3 concentrations of 0 mM, 3 mM, 6 mM and 12 mM, the salt KCl removal efficiency was respectively 10.84%, 40.67%, 47.67% and 57.16% within 30 min charging process, and the system still did not reach equilibrium. Taking 12 mM KI_3 for example, the average salt removal rate during electrosorption was enhanced by 427% as a result of the addition of KI_3 to the cathodic flow-electrode. Nevertheless, when the initial KI_3 concentrations further increased to 18 mM, it was noticed that the desalination performance only increased a little. The reason is that application of two flow-electrodes with equal volume and carbon loading but with I_3^-/I^- redox couple in the cathodic chamber is expected to be limited by the salt adsorption capacity of the flowing anode. The desalination performance of FCDI under different cathodic KI_3 concentrations was proportional to the electrical current flowing through the FCDI cell at a fixed charging voltage with an increase in initial KI_3 concentrations leading to a larger current along with similar increase amplitude to that of desalting efficiency (Fig. 2b).

For comparison, we also investigated the desalination performance of FCDI with cathodic flow-electrode initially consisting of 1000 mg L^{-1} KCl and 12 mM KI_3 (termed “Redox” group). From Fig. S6, we can know that the “Redox” group performed better in salt removal than the “Carbon” group (i.e., cathodic flow-electrode initially consisting of 5 wt % activated carbon, 1 wt% carbon black and 1000 mg L^{-1} KCl), but was still far inferior to the “Carbon + Redox” group (i.e., cathodic flow-electrode initially consisting of 5 wt% activated carbon, 1 wt% carbon black, 1000 mg L^{-1} KCl and 12 mM KI_3), which suggests that there is a good synergistic effect between the carbons and the iodide redox couple in desalination. Apart from the effects of initial KI_3 concentrations in the cathodic flow-electrode, we also studied the influence of operating voltages on the salt removal process in the presence of KI_3 (see Fig. S7). As expected, a higher applied voltage ranging from 0.9 V to 1.8 V contributed to an increased rate of change in conductivity of the treated salty water during both electrosorption and desorption, correspondingly with a larger electrical current flowing through the FCDI cell. As both anodic and cathodic flow-electrodes initially contained 1000 mg L^{-1} KCl at the time of preparation, more KCl could move through the ion exchange membranes and enter the treated water during desorption stage compared to electrosorption stage, thereby causing a higher conductivity of the treated water than the initial conductivity at the end of desorption. In addition, it was observed that the pH of the treated water and the pH in the anodic and cathodic flow-electrodes varied insignificantly (Figs. S8 and S9).

To understand the underlying mechanisms involved in the

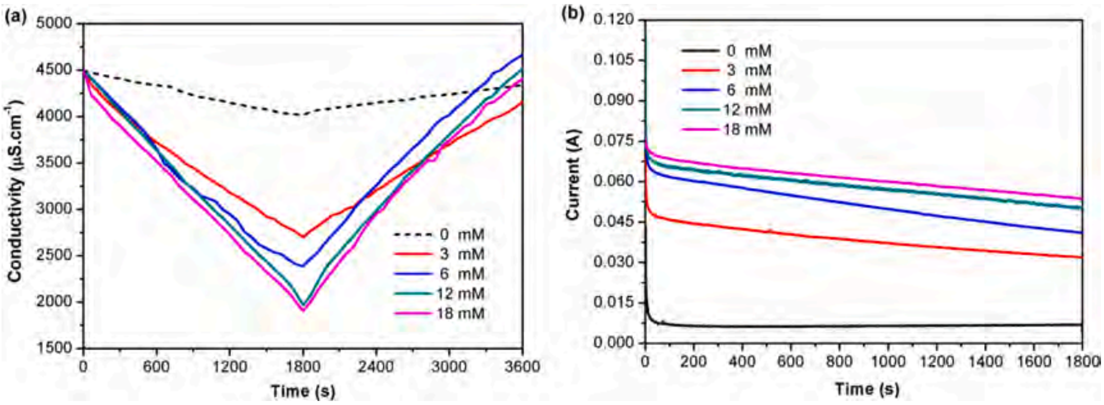

Fig. 2. (a) Dynamic variation in conductivity of the treated salty water during electrosorption and desorption, and (b) variation of current during electrosorption under different initial KI_3 concentrations in the cathodic flow-electrode. The anodic flow-electrode initially consisted of 5 wt% activated carbon, 1 wt% carbon black and 1000 mg L^{-1} KCl, while the cathodic flow-electrode initially consisted of 5 wt% activated carbon, 1 wt% carbon black, 1000 mg L^{-1} KCl and certain concentrations (0, 3, 6, 12, 18 mM) of KI_3; Feed solution: 3000 mg L^{-1} KCl; Charging voltage: 1.2 V; Discharging voltage: −1.2 V.

significantly enhanced desalination performance of FCDI via introduction of KI_3 in the cathodic flow-electrode, we carried out CV analysis and EIS measurement for the types of "Carbon" and "Carbon + Redox" electrodes, and monitored the temporal variation of the aqueous I^- concentration in the cathodic flow-electrode. As can be seen from Fig. 3a, when KI_3 existed in the flow-electrode, the CV curve showed a clear pair of oxidation/reduction peaks around + 0.75 and + 0.1 V (vs. Ag/AgCl) in the selected potential range, whereas, in the absence of the iodide redox couple, the CV curve exhibited a typical capacitor-like characteristic with a symmetric cyclic shape. Combined with the results displayed in Figs. 2 and S6, it can be inferred that, after addition of KI_3, electrochemical redox reactions in the cathodic flow-electrode also play an important role in the FCDI desalination and salination processes apart from the carbon electric-double-layer interaction. During charging (i.e., electrosorption), in the cathodic chamber of FCDI, I_3^- can be reduced to I^-, as described by the following reaction:

Reduction: $I_3^- + 2e^- \rightarrow 3I^-$ (2)

During discharging (i.e., desorption), I^- can be oxidized to I_3^- as follows:

Oxidation: $3I^- \rightarrow I_3^- + 2e^-$ (3)

Due to charge neutralization in the cathodic electrolyte, ideally, two K^+ ions in the feed water would transport through the CEM entering the cathodic chamber of FCDI once one I_3^- ion was reduced during electrosorption thereby favoring desalination of the feedwater stream. The anodic flow-electrode accomplished the uptake of an increased number of Cl^- in order to preserve the electro-neutrality of the global electrolyte. During desorption, the reverse process would occur, as illustrated in Fig. 4. The associated ion removal/release mechanism was further supported by temporal variation of the aqueous I^- concentration in the cathodic flow-electrode. Aqueous I^- concentration in the cathodic flow-electrode increased during charging and decreased during discharging, as shown in Fig. 3b.

EIS measurements were performed for types of "Carbon" and "Carbon + Redox" electrodes to understand how KI_3 additive affected flow-electrode internal resistance and conductivity. From the Nyquist plots presented in Fig. 3c, we can know that the ohmic resistance across the electrolyte (revealed by intersection of the curves on the x-axis) and the charge transfer resistance between carbon particles and between carbon particle and current collector (suggested by the radius of semicircle) of "Carbon + Redox" electrode were both lower than those of "Carbon" electrode, implying that the presence of KI_3 could benefit ion transport and charge transfer, leading to enhancement of the salt removal rate. Fig. 3d presents the amount of K^+ in the aqueous phase of cathodic flow-electrode excluding the original value and amount of K^+ adsorbed on the carbons of cathodic flow-electrode at the end of electrosorption in the case of different initial cathodic KI_3 concentrations, from which it can be known that introduction of KI_3 into the cathodic flow-electrode facilitated salt removal enabled via iodide redox reactions and simultaneously via carbon adsorption, although the promoting degree for carbon adsorption was not remarkable.

For practical use of this method as described here, good regeneration and stable cycling behavior is of great importance. We evaluated this characteristic by conducting both salt electrosorption and desorption processes over twenty consecutive cycles for the types of "Carbon" and

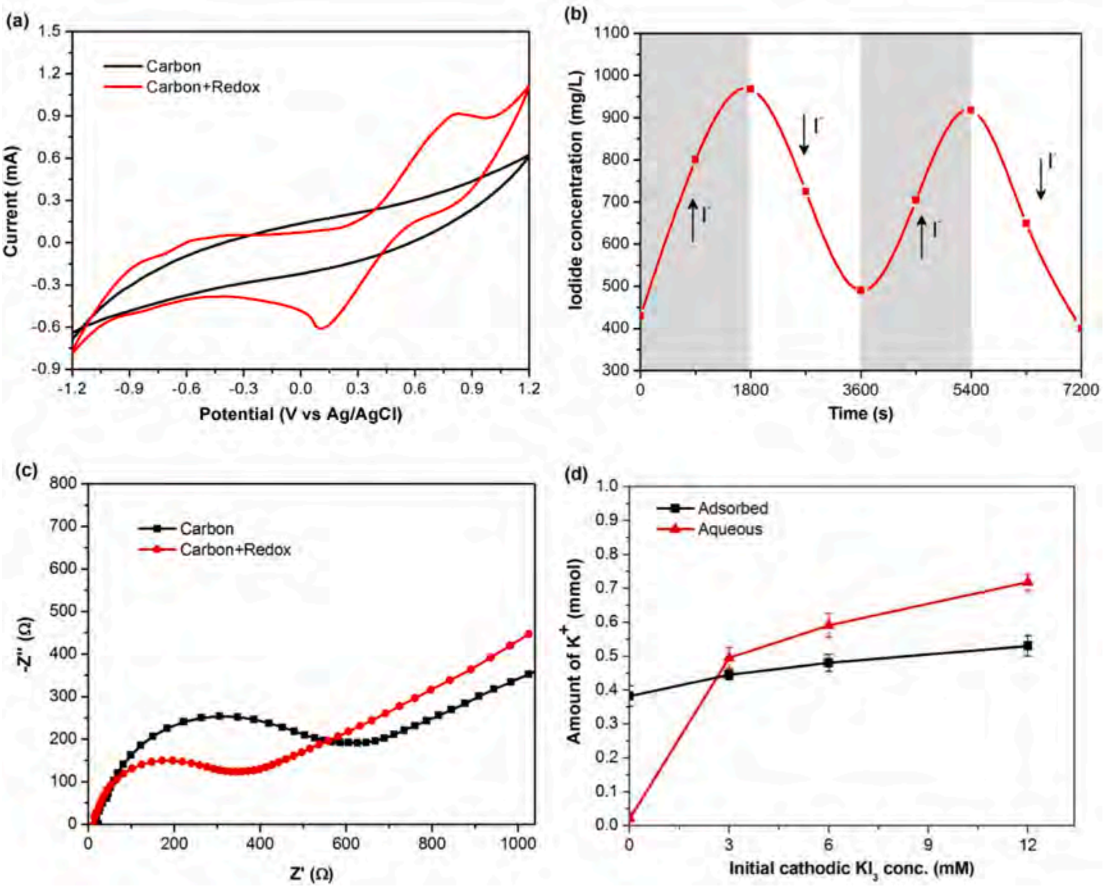

Fig. 3. (a) CV curves and (c) EIS data measured in a beaker cell for the types of "Carbon" and "Carbon + Redox" electrodes; (b) temporal variation of the aqueous I^- concentration in the cathodic flow-electrode under experimental conditions of initial 12 mM KI_3, 3000 mg L^{-1} KCl feed solution, ±1.2 V operating voltage, and (d) amount of K^+ in the aqueous phase of cathodic flow-electrode excluding the original value and amount of K^+ adsorbed on the carbons of cathodic flow-electrode at the end of electrosorption in the case of different initial cathodic KI_3 concentrations.

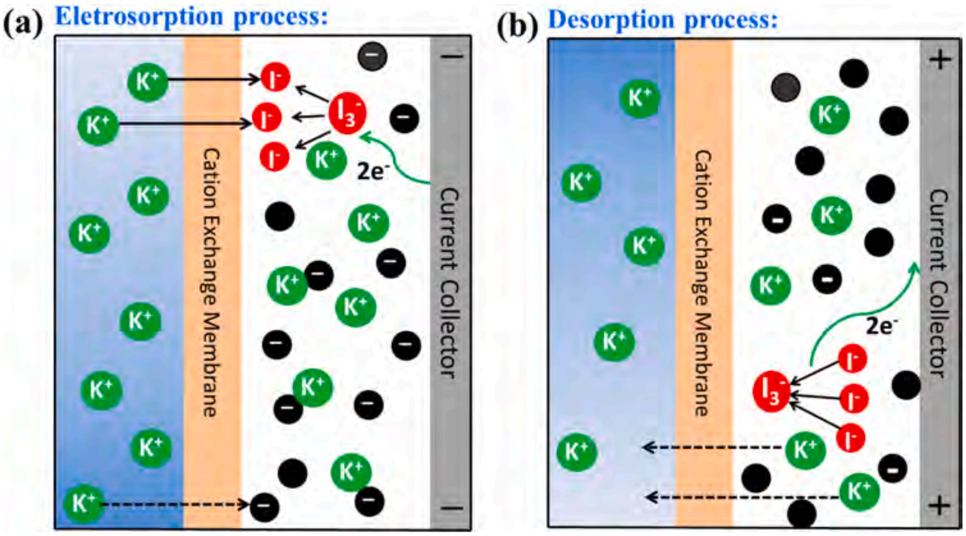

Fig. 4. Schematic of the (a) electrosorption and (b) desorption processes in FCDI with cathodic flow-electrode introduced with KI_3.

"Carbon + Redox" electrodes, as displayed in Fig. 5. In the first cycle, for the type of "Carbon" electrode, the conductivity dropped from initial 4500 μS/cm to 4020μS/cm during 30-min charging, and then increased to 4360 μS/cm during 30-min discharging. The second cycle saw the readsorption of salt released during the first cycle and another redesorption with the following cycles behaving similar to the second cycle. By contrast, for the type of "Carbon + Redox" electrode, in the first cycle, a much more rapid salt removal occurred during 30-min charging with a complete desorption of the adsorbed salt during 30-min discharging, and the following cycles presented similar profiles to the first cycle. To sum up, the cycling behavior of FCDI with cathodic flow-electrode introduced with KI_3 exhibited a high stability without decay in the desalination efficiency and recuperability after twenty successive runs, suggesting that the proposed approach would be suitable for multi-cycle desalination of saline feed streams.

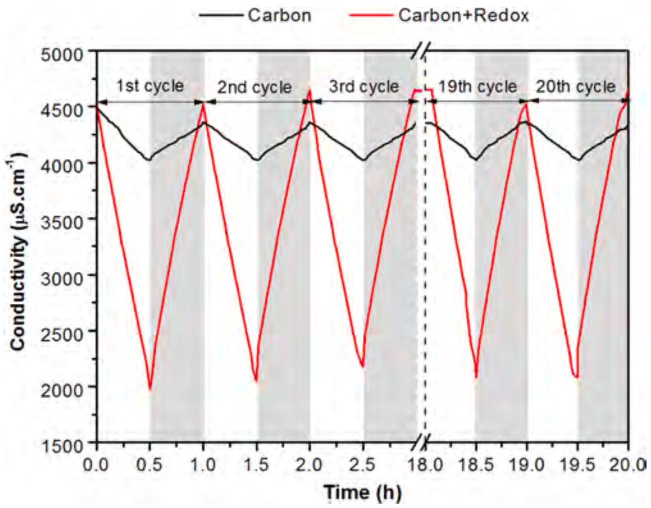

Fig. 5. The cycling (electrosorption and desorption) behavior of FCDI for the types of "Carbon" and "Carbon + Redox" electrodes over twenty consecutive cycles. Initial KI_3 concentration: 12 mM; Feed solution: 3000 mg L^{-1} KCl; Charging voltage: 1.2 V; Discharging voltage: −1.2 V.

3.3. *Potential in treatment of iodide-containing saline wastewater*

Although the commercial cation exchange membrane (CEM) could inhibit the diffusion of cathodic I^-/I_3^- couple into the treated water stream, consideration should be given to the possible release or leakage of I^-/I_3^- through the ion-exchange membrane and into the treated water. As such, we measured the concentration of total iodine in the treated water by ICP-MS at the end of electrosorption, and it was found that the total iodine concentration was 2.6 mg/L when cathodic flow-electrode was introduced with 12 mM KI_3 at an operating voltage of 1.2 V, which was the largest for all the different KI_3 concentrations examined (for information, a document from the World Health Organization reveals that, in a five-year study, no serious health issue occurred for people consuming water with an iodide concentration of 1 mg/L). Considering the potential environmental and health risks, and given that the approach proposed herein is not necessarily applied to the generation of potable water, we explored the feasibility of this method in treatment of iodide-containing saline wastewater.

Fig. 6 shows the removal efficiencies of Cl^-, Br^-, NO_3^-, SO_4^{2-}, total iodine from feed water when treating iodide-containing saline wastewater (1000 mg/L Cl^-, 100 mg/L Br^-, 100 mg/L NO_3^-, 100 mg/L SO_4^{2-}, 10 mg/L I^-) by FCDI with cathodic flow-electrode introduced with 12 mM KI_3 for 30 min electrosorption time under 1.2 V charging. It is apparent that the removal efficiencies of Cl^-, Br^-, NO_3^-, SO_4^{2-}, total iodine were all enhanced significantly when the cathodic chamber of FCDI was added with KI_3, with this remarkable ion removal performance achieved without causing secondary pollution. Particularly, the total iodine in the feed water decreased from 10 mg/L to 5.5 mg/L after 30-minute treatment regardless of the possible release or leakage of I^-/I_3^- into the treated water. To conclude, such an approach will open a new door for realizing excellent treatment of iodide-containing saline wastewater.

4. Conclusions

In this work, we have demonstrated that introduction of KI_3 into the cathodic flow-electrode could greatly improve the desalination performance of FCDI operated in isolated closed-cycle mode with a similar positive effect noticed during desorption upon polarity reversal. Additionally, the salt removal rate increased with an increase in the initial concentration of KI_3 in the cathodic flow-electrode and an increase in the applied voltage. The excellent ion removal performance resulted from the good synergistic effect between the carbons (via electric-double-layer electrostatic interaction) and the iodide redox couple (via electrochemical redox reactions) rather than the elevated cathodic electrolyte conductivity induced by the addition of KI_3. Although a concern arose from the possible minor release or leakage of I^-/I_3^- into

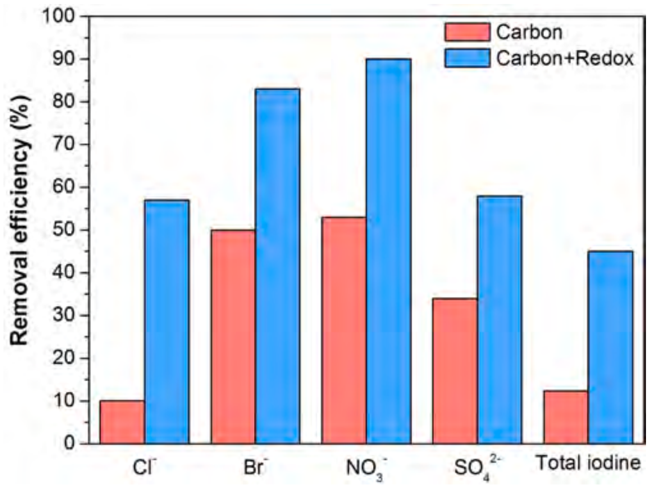

Fig. 6. Removal efficiencies of Cl^-, Br^-, NO_3^-, SO_4^{2-}, total iodine when treating iodide-containing saline wastewater by FCDI for the types of "Carbon" and "Carbon + Redox" electrodes. Initial KI_3 concentration: 12 mM; Applied voltage: 1.2 V; Electrosorption time: 30 min.

the treated water, and therefore the proposed approach may not be suitable for the generation of potable water, the results of the present study clearly showed that this innovation holds great promise in the treatment of iodide-containing saline wastewater. In spite of such a breakthrough, ongoing efforts are required to further improve and perfect the system by adopting permselective membranes that are less permeable to I^-/I_3^-, finding safer and more environment-friendly cathodic redox couples, or additionally introducing proper redox couples for the anodic flow-electrode to maximize ion removal.

Declaration of Competing Interest

The authors declare that they have no known competing financial interests or personal relationships that could have appeared to influence the work reported in this paper.

Acknowledgements

This study was financially supported by the National Natural Science Foundation of China (51809088), the Funds for Innovative Province Construction of Hunan Province of China (2019RS1025), and the Fundamental Research Funds for the Central Universities (531118010106).

Appendix A. Supplementary data

Ancillary experimental results and discussion are available in the Supporting Information. Supplementary data to this article can be found online at https://doi.org/10.1016/j.cej.2021.129905.

References

[1] A. Arenas-Sánchez, A. Rico, M. Vighi, Effects of water scarcity and chemical pollution in aquatic ecosystems: State of the art, Sci. Total Environ. 572 (2016) 390–403.

[2] W. Xing, J. Liang, W. Tang, D. He, M. Yan, X. Wang, Y. Luo, N. Tang, M. Huang, Versatile applications of capacitive deionization (CDI)-based technologies, Desalination 482 (2020) 114390.

[3] C. Liang, H.-Y. Niu, H. Guo, C.-G. Niu, Y.-Y. Yang, H.-Y. Liu, W.-W. Tang, H.-P. Feng, Efficient photocatalytic nitrogen fixation to ammonia over bismuth monoxide quantum dots-modified defective ultrathin graphitic carbon nitride, Chem. Eng. J. 406 (2021) 126868.

[4] K. Fang, H. Gong, W. He, F. Peng, C. He, K. Wang, Recovering ammonia from municipal wastewater by flow-electrode capacitive deionization, Chem. Eng. J. 348 (2018) 301–309.

[5] W. Xing, J. Liang, W. Tang, G. Zeng, X. Wang, X. Li, L. Jiang, Y. Luo, X. Li, N. Tang, M. Huang, Perchlorate removal from brackish water by capacitive deionization: Experimental and theoretical investigations, Chem. Eng. J. 361 (2019) 209–218.

[6] M. Mao, T. Yan, G. Chen, J. Zhang, L. Shi, D. Zhang, Selective capacitive removal of Pb^{2+} from wastewater over redox-active electrodes, Environ. Sci. Technol. 55 (1) (2021) 730–737.

[7] O. Pastushok, F. Zhao, D.L. Ramasamy, M. Sillanpää, Nitrate removal and recovery by capacitive deionization (CDI), Chem. Eng. J. 375 (2019) 121943.

[8] J. Ai, J. Li, K. Li, F. Yu, J. Ma, Highly flexible, self-healable and conductive poly (vinyl alcohol)/$Ti_3C_2T_x$ MXene film and its application in capacitive deionization, Chem. Eng. J. 408 (2021) 127256.

[9] J. Ma, C. Zhang, F. Yang, X. Zhang, M.E. Suss, X. Huang, P. Liang, Carbon black flow electrode enhanced electrochemical desalination using single-cycle operation, Environ. Sci. Technol. 54 (2) (2020) 1177–1185.

[10] W. Xing, M. Zhang, J. Liang, W. Tang, P. Li, Y. Luo, N. Tang, J. Guo, Facile synthesis of pinecone biomass-derived phosphorus-doping porous carbon electrodes for efficient electrochemical salt removal, Sep. Purif. Technol. 251 (2020) 117357.

[11] L.i. Wang, Y. Liang, L.i. Zhang, Enhancing performance of capacitive deionization with polyelectrolyte-infiltrated electrodes: Theory and experimental validation, Environ. Sci. Technol. 54 (9) (2020) 5874–5883.

[12] S. Tian, J. Wu, X. Zhang, K. Ostrikov, Z. Zhang, Capacitive deionization with nitrogen-doped highly ordered mesoporous carbon electrodes, Chem. Eng. J. 380 (2020) 122514.

[13] X. Xu, T. Yang, Q. Zhang, W. Xia, Z. Ding, K. Eid, A.M. Abdullah, M. Shahriar, A. Hossain, S. Zhang, J. Tang, L. Pan, Y. Yamauchi, Ultrahigh capacitive deionization performance by 3D interconnected MOF-derived nitrogen-doped carbon tubes, Chem. Eng. J. 390 (2020) 124493.

[14] C. Zhang, D.i. He, J. Ma, W. Tang, T.D. Waite, Faradaic reactions in capacitive deionization (CDI) - problems and possibilities: A review, Water Res. 128 (2018) 314–330.

[15] Z. Chen, X. Xu, Z. Ding, K. Wang, X. Sun, T. Lu, M. Konarova, M. Eguchi, J. G. Shapter, L. Pan, Y. Yamauchi, Ti_3C_2 MXenes-derived $NaTi_2(PO_4)_3$/MXene nanohybrid for fast and efficient hybrid capacitive deionization performance, Chem. Eng. J. 407 (2021) 127148.

[16] Y. Liu, X. Gao, Z. Wang, K. Wang, X. Dou, H. Zhu, X. Yuan, L. Pan, Controlled synthesis of bismuth oxychloride-carbon nanofiber hybrid materials as highly efficient electrodes for rocking-chair capacitive deionization, Chem. Eng. J. 403 (2021) 126326.

[17] S.I. Jeon, H.R. Park, J.G. Yeo, S. Yang, C.H. Cho, M.H. Han, D.K. Kim, Desalination via a new membrane capacitive deionization process utilizing flow-electrodes, Energy Environ. Sci 6 (2013) 1471.

[18] K. Luo, Q. Niu, Y. Zhu, B. Song, G. Zeng, W. Tang, S. Ye, J. Zhang, M. Duan, W. Xing, Desalination behavior and performance of flow-electrode capacitive deionization under various operational modes, Chem. Eng. J. 389 (2020) 124051.

[19] W. Tang, J. Liang, D. He, J. Gong, L. Tang, Z. Liu, D. Wang, G. Zeng, Various cell architectures of capacitive deionization: Recent advances and future trends, Water Res. 150 (2019) 225–251.

[20] A. Rommerskirchen, Y. Gendel, M. Wessling, Single module flow-electrode capacitive deionization for continuous water desalination, Electrochem. Commun. 60 (2015) 34–37.

[21] C. Zhang, J. Ma, L. Wu, J. Sun, L. Wang, T. Li, T.D. Waite, Flow electrode capacitive deionization (FCDI): recent developments, environmental applications, and future perspectives, Environ. Sci. Technol. 2021, in press, Doi: 10.1021/acs.est.0c06552.

[22] P. Nativ, Y. Badash, Y. Gendel, New insights into the mechanism of flow-electrode capacitive deionization, Electrochem. Commun. 76 (2017) 24–28.

[23] J. Wang, J. Dai, Z. Jiang, B. Chu, F. Chen, Recent progress and prospect of flow-electrode electrochemical desalination system, Desalination 504 (2021) 114964.

[24] L. Wang, C. Zhang, C. He, T.D. Waite, S. Lin, Equivalent film-electrode model for flow-electrode capacitive deionization: Experimental validation and performance analysis, Water Res. 181 (2020) 115917.

[25] Y. Cho, C.-Y. Yoo, S.W. Lee, H. Yoon, K.S. Lee, S. Yang, D.K. Kim, Flow-electrode capacitive deionization with highly enhanced salt removal performance utilizing high-aspect ratio functionalized carbon nanotubes, Water Res. 151 (2019) 252–259.

[26] G.J. Doornbusch, J.E. Dykstra, P.M. Biesheuvel, M.E. Suss, Fluidized bed electrodes with high carbon loading for water desalination by capacitive deionization, J. Mater. Chem. A 4 (10) (2016) 3642–3647.

[27] H.-R. Park, J. Choi, S. Yang, S.J. Kwak, S.-i. Jeon, M.H. Han, D.K. Kim, Surface-modified spherical activated carbon for high carbon loading and its desalting performance in flow-electrode capacitive deionization, RSC Adv. 6 (74) (2016) 69720–69727.

[28] J.W. Campos, M. Beidaghi, K.B. Hatzell, C.R. Dennison, B. Musci, V. Presser, E. C. Kumbur, Y. Gogotsi, Investigation of carbon materials for use as a flowable electrode in electrochemical flow capacitors, Electrochim. Acta 98 (2013) 123–130.

[29] P. Liang, X. Sun, Y. Bian, H. Zhang, X. Yang, Y. Jiang, P. Liu, X. Huang, Optimized desalination performance of high voltage flow-electrode capacitive deionization by adding carbon black in flow-electrode, Desalination 420 (2017) 63–69.

[30] K.B. Hatzell, M.C. Hatzell, K.M. Cook, M. Boota, G.M. Housel, A. McBride, E. C. Kumbur, Y. Gogotsi, Effect of oxidation of carbon material on suspension electrodes for flow electrode capacitive deionization, Environ. Sci. Technol. 49 (5) (2015) 3040–3047.

[31] S. Yang, J. Choi, J.-g. Yeo, S.-i. Jeon, H.-R. Park, D.K. Kim, Flow-electrode capacitive deionization using an aqueous electrolyte with a high salt concentration, Environ. Sci. Technol. 50 (11) (2016) 5892–5899.

[32] J. Ma, D.i. He, W. Tang, P. Kovalsky, C. He, C. Zhang, T.D. Waite, Development of redox-active flow electrodes for high-performance capacitive deionization, Environ. Sci. Technol. 50 (24) (2016) 13495–13501.

[33] Z. Wang, Y. Hu, Q. Wei, W. Li, X. Liu, F. Chen, Enhanced desalination performance of a flow-electrode capacitive deionization system by adding vanadium redox couples and carbon nanotubes, J. Phys, Chem. C 125 (2021) 1234–1239.

[34] Q. Li, Y. Zheng, D. Xiao, T. Or, R. Gao, Z. Li, M. Feng, L. Shui, G. Zhou, X. Wang, Z. Chen, Faradaic electrodes open a new era for capacitive deionization, Adv. Sci. 7 (2020) 2002213.

[35] J. Lee, P. Srimuk, S. Fleischmann, X. Su, T.A. Hatton, V. Presser, Redox-electrolytes for non-flow electrochemical energy storage: A critical review and best practice, Prog. Mater. Sci. 101 (2019) 46–89.

[36] J. Lee, P. Srimuk, S. Carpier, J. Choi, R.L. Zornitta, C. Kim, M. Aslan, V. Presser, Confined redox reactions of iodide in carbon nanopores for fast and energy-efficient desalination of brackish water and seawater, ChemSusChem 11 (19) (2018) 3460–3472.

[37] J. Lee, P. Srimuk, R.L. Zornitta, M. Aslan, B.L. Mehdi, V. Presser, High electrochemical seawater desalination performance enabled by an iodide redox electrolyte paired with a sodium superionic conductor, ACS Sustain. Chem. Eng. 7 (11) (2019) 10132–10142.